JOC The Journal of Organic Chemistry

Article

Water Soluble Naphthalene Diimides as Singlet Oxygen Sensitizers

Filippo Doria, Ilse Manet, Vincenzo Grande, Sandra Monti, and Mauro Freccero

J. Org. Chem., **Just Accepted Manuscript** • Publication Date (Web): 19 Jul 2013

The Journal of Organic Chemistry is published by the American Chemical Society.
1155 Sixteenth Street N.W., Washington, DC 20036

Water Soluble Naphthalene Diimides as Singlet Oxygen Sensitizers

Filippo Doria,[a] *Ilse Manet,*[b]* *Vincenzo Grande,*[a] *Sandra Monti,*[b] *and Mauro Freccero*[a]*

[a]Dipartimento di Chimica, Università di Pavia. V.le Taramelli 10, 27100 Pavia, Italy.

[b]Istituto per la Sintesi Organica e la Fotoreattività, Consiglio Nazionale delle Ricerche, via Gobetti 101, 40129 Bologna, Italy

mauro.freccero@unipv.it

ilse.manet@isof.cnr.it

Hydrosoluble naphthalene diimides exhibiting multimodal photophysical and photochemical properties.

TOC

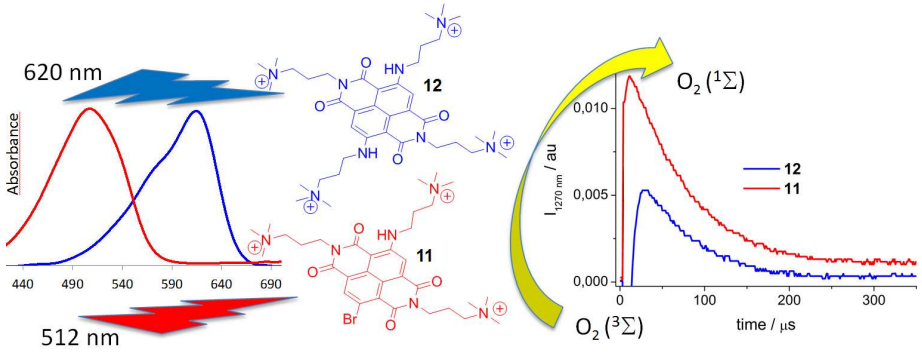

Abstract: Br and/or alkylammino substituted and hydrosoluble naphthalene diimides (NDIs) were synthesized to study their multimodal photophysical and photochemical properties. Br containing NDIs (i.e., **11**) behaved as both singlet oxygen ($^1O_2$) photosensitizers, and fluorescent molecules, upon irradiation at 532 nm. Among the NDIs not containing Br, only **12** exhibited similar photophysical properties to Br-NDIs, by irradiation above 610 nm, suggesting that for these NDIs both singlet and triplet excited state properties are strongly affected by length, structure of the solubilizing moieties and pH of the solution. Laser flash photolysis confirmed that the NDI lowest triplet excited state was efficiently populated, upon excitation at both 355 and 532 nm, and that free amine moieties quenched both the singlet and triplet excited states by intramolecular electron transfer, with generation of detectable radical anions. Time-resolved experiments, monitoring the 1270 nm $^1O_2$ phosphorescence decay generated upon laser irradiation at 532 nm, allowed a ranking of the NDIs as sensitizers, based on their $^1O_2$ quantum yields (Φ_Δ). The tetra-functionalized **12**, exhibiting a long-lived triplet state ($\tau \sim 32$ µs) and the most promising absorptivity for photodynamic therapy application, was tested as efficient photosensitizers in the photo-oxidations of 1,5-dihydroxylnaphthalene and 9,10-anthracenedipropionic acid in acetonitrile and water.

Introduction

Photodynamic therapy (PDT) is based on the use of a light-activatable chemical, called photosensitizer (PS), and irradiation with light of appropriate wavelength to impart cytotoxicity via the generation of reactive molecular species.[1-3] Typically, the useful range of wavelengths for therapeutic activation of the PS is 600-800 nm in order to optimize tissue penetration. The main process occurring upon excitation of the photosensitizer is the formation of the PS triplet excited state and energy transfer to molecular oxygen yielding singlet oxygen ($^1O_2$),[4] a very cytotoxic species. It is important to stress that photosensitizers that preserve their fluorescence, due to incomplete singlet-triplet intersystem crossing (ISC), can act also as fluorescent agents enabling *contemporarily* localization of the PS in the biological tissue and occurrence of the therapeutic action.[5] This is a very appealing objective in the frame of multimodal theranostic applications.

The triplet sensitizers actually used for PDT are limited to transition-metal complexes of porphyrinoids, reduced porphyrins and phthalocyanines with high ISC efficiency due to the heavy atom effect of the transition metal.[2,3,6-8] Among their main drawbacks are low solubility and tendency to aggregate in aqueous environment leading to non radiative decay pathways of their excited states and consequently inefficient energy transfer to oxygen. More recently, porphyrin-like photosensitizers have been included by or bound covalently to nanoparticles with size dimension in the nanometer range to optimize delivery and $^1O_2$ formation.[9,10] Even though nano-sized delivery systems for photosensitizers offer several advantages, they suffer from drawbacks due to their complexity and often lower efficiency in the $^1O_2$ generation. Therefore the design and synthesis of water soluble organic triplet sensitizers with intense absorption of red light, high photochemical stability and a long-lived triplet excited state is still an interesting issue, particularly because very few have been reported yet. Recently, a bodipy-based triplet sensitizers soluble in water has been described as singlet oxygen sensitizer exhibiting anyway a rather low efficiency (yield in $^1O_2$, 10%).[11] During the last years, our attention has been focused on naphthalene diimides (NDIs) and core-substituted NDIs[12] as selective nucleic acids (NAs) ligands and

fluorescent probes. In more detail, Neidle's group and our research unit have shown that tri- and tetra-substituted NDIs are potent and reversible ligands[13-15] as well as alkylating agents targeting guanine rich NAs folded into G-quadruplex structures (G4s).[16-19] G-rich sequences able to fold into G4 are present in biologically relevant proto-oncogenes and oncogenes promoters (like *c-kit* and *c-myc*)[20-22] as well as human telomeres and participate in biological processes crucial for cell replication and survival.[21,23] Consequently they represent a very appealing target and propelled the research for the development of new therapeutic approaches based on their selective targeting. Interestingly, the optoelectronic properties of the NDI core can be effectively tuned by substitution,[24-26] as electron rich substituents on the aromatic core give origin to strong absorption and emission in the red spectroscopic window useful for PDT applications. In addition, the NDI's binding properties toward G4s[14,17] may also be exploited for potential selective photocleavage as suggested recently for cationic Zn-phthalocyanines.[27] This prompted us to start from the NDI core carrying amine substituents on the naphthalene unit to engineer efficient water soluble $^1O_2$ photosensitizers, by structural modifications.

Results and Discussion

Design and synthesis. In this work we have designed and synthesised a class of water soluble NDIs (Table 1) with unique optoelectronic properties that can be used as efficient water-soluble singlet oxygen photosensitizers, and fluorescent probes.

Table 1. Structures of the water soluble NDIs (**1**-**12**) investigated as singlet oxygen sensitizers.

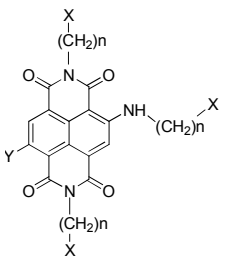

n	Y	X=NMe$_2$	X=NMe$_3^+$Cl$^-$
2	H	**1**	**7**
	Br	**2**	**8**
	NH(CH$_2$)$_2$X	**3**	**9**
3	H	**4**	**10**
	Br	**5**	**11**
	NH(CH$_2$)$_3$X	**6**	**12**

To synthesize the above tri- and tetra-substituted NDIs sketched in Table 1, we followed two different three-steps synthetic protocols. The commercially available anhydride was brominated with dibromocyanuric acid and the resulting product mixture containing the 2,6-dibromo-1,4,5,8-naphthalenetetracarboxylic acid dianhydride (**13**) was used for a classical imidation procedure under acidic condition yielding the 2,6-dibromo-substituted NDIs **14**–**15** [step (a) in the Scheme 1].[28,29]

SCHEME 1. Synthesis of water soluble tri- and tetra-substituted NDIs. a) N^1,N^1-dimethylethane-1,2-diamine (n=2) or N^1,N^1-dimethylpropane-1,3-diamine (n=3) in acetic acid, 90°C, 30 min, under N_2; 43% yield; b) N^1,N^1-dimethylethane-1,2-diamine (n=2) or N^1,N^1-dimethylpropane-1,3-diamine (n=3), acetonitrile, 70 °C, 4 h; c) N^1,N^1-dimethylethane-1,2-diamine (n=2) or N^1,N^1-dimethylpropane-1,3-diamine (n=3), dry DMF, 135°C, 3 min; MW assisted and closed vessel synthesis; d) MeI, acetonitrile, r. t., 16 h.

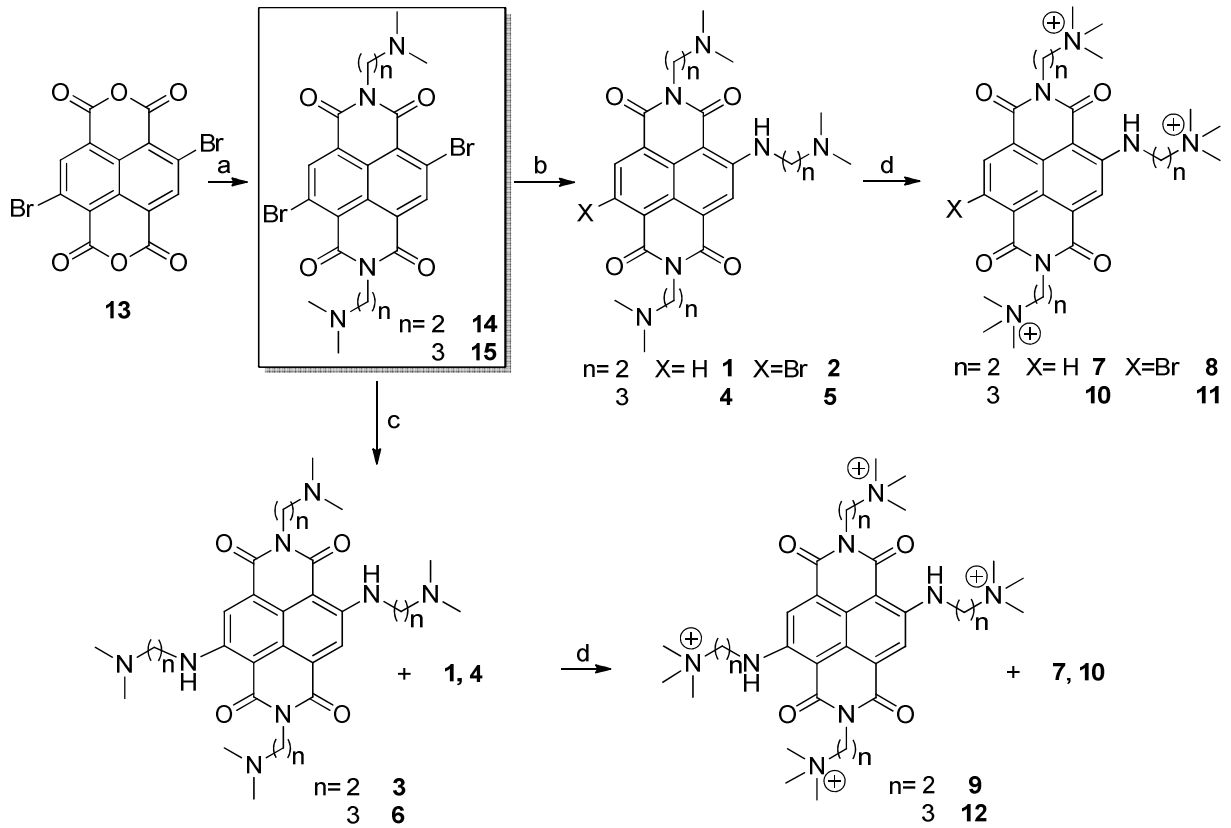

The following nucleophilic aromatic substitution (S_NAr) is the key step of the whole synthetic

protocol. Recently, regioselectivity of the S_NAr on poly-bromosubstituted NDIs with aniline has been successfully achieved in the presence of fluoride.[30] The choice between two different conditions [(b) and (c), Scheme 1] allows to discriminate the reactivity of the aromatic core, yielding mainly mono- (c) or di-functionalization (b). To synthetize the tetra-substituted NDIs (**3**, **6**) in good yields, we performed a one-pot microwave-assisted (MW) functionalization in DMF at 135°C for 3 minutes, in close-vessel. Differently, the mono-substitutions were obtained under milder conditions in acetonitrile at 70°C for 4h using N^1,N^1-dimethylethane-1,2-diamine, or N^1,N^1-dimethylpropane-1,3-diamine. Under these milder conditions only regioselective mono-functionalization of the 2,6-dibromo-NDIs was efficiently achieved to give mainly the new Br-derivatives **2**, and **5**. These Br-NDIs were prepared in order to improve intersystem crossing by the presence of the heavy atom and efficiently populate the triplet excited state.[31] In addition, in order to increase the lifetime of both the singlet and triplet excited states, inhibiting their deactivation by intra-molecular electron Transfer (eT) quenching, the corresponding quaternary ammonium salts **7**-**12** have been synthesized.

The quaternary ammonium salts **7**-**12** were synthesized by exhaustive methylation of the corresponding amines **1**-**6**, and subsequently purified by HPLC as trifluoroacetate salts. For the NDIs embedding the ethylene spacer (**1**-**3**), the reaction carried out in acetonitrile with an excess of methyl iodide gave the desired products **7**-**9** with quantitative yields after 24 h at r.t. Following the same strategy for the NDIs with the propyl amine substituents (**4**-**6**), a mixture of quaternary ammonium salts partially methylated, were obtained. In order to get the NDIs **10**-**12** a suspension of sodium carbonate was required to achieve quantitative conversion. Such a difference in reactivity is likely the result of a different basicity of the amines. All the NDIs **1**-**12** have been purified by HPLC using ACN:H_2O + 0.1% CF_3COOH, and characterized as chloride salts.

Photophysical characterization: Figures 1a and 1b show the absorption and corrected fluorescence spectra of the NDI quaternary ammonium salts **7**-**12** (Scheme 1).

Figure 1. UV-vis absorption (solid lines) and fluorescence spectra (dotted lines) of the NDIs (a) **7-9** and (b) **10-12**. Excitation at 485 nm and 600 nm for **7**, **8**, **10**, **11** and **9**, **12**, respectively (1 cm path length).

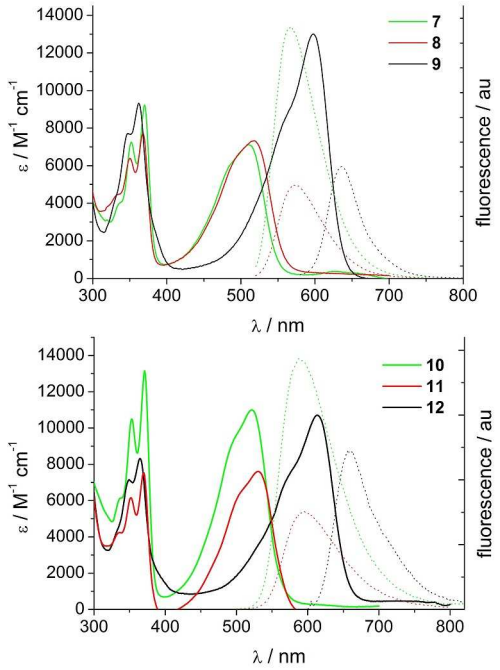

The absorption spectra of the amines (**1-6**) in solutions of different pH are very similar to those of the quaternary ammonium salts, so the protonation state of the terminal amine groups (NMe_2) does not influence the absorption spectra (see Supp. Inf.). The absorption band with vibronic signature in the 300-400 nm range is typical of the NDI core, and is not substantially affected by substitution.[32] It clearly emerges how the introduction of just one amine substituent is able to generate a second absorption band in the visible of comparable intensity to that with maximum at 370 nm.

Compared to the H-derivative bromination of the NDI core shifts the absorption band in the visible spectrum to the red by ca. 10 nm, due to the Br atom acting as weak electron donating substituent. The most significant shift of ca. 90 nm is anyway obtained by introduction of the second amine substituent on the NDI core. With the introduction of the second amine substituent the NDI derivative complies with the PDT requirements of strong absorption in the 600-800 nm spectroscopic window. As underlined in several studies these interesting electronic properties arise from a charge transfer (CT)

transition involving the doublet of the aromatic amines.[25,33]

Table 2 collects the photophysical data of all the quaternary ammonium salts (**7**-**12**), in water, and their related amines (**1**-**6**), under acid buffered conditions. Measurements were carried out under acidic conditions in an attempt to protonate all terminal amine groups. Protonation of the aromatic amines was negligible at pH above 1, as the absorption spectra did not change (see Supp. Inf.).

Table 2. Photophysical properties of the NDI compounds in water for the salt derivatives in phosphate buffer of pH 2 for the neutral derivatives.

NDIs	λ_{max} (nm)	ε_{max} ($M^{-1}cm^{-1}$)	Φ_F [a]	τ_f (ns)[b]	Φ_Δ [c]	τ_T (μs)[d]
4	522	11000	0.19	5.60	-	-
10	522	11000	0.21	5.50	-	0.34
1	509	7100	0.29	7.36	-	-
7	511	7100	0.29	7.35	-	0.18
6	616	7400	0.17	4.40	-	-
12	613	10700	0.17	4.00	0.30	32
3	598	13000	0.26	7.00	0.04	-
9	598	13000	0.27	7.10	0.07	7.4
5	531	6400	0.11	3.50	0.39	26
11	530	7600	0.12	3.33	0.46	22
2	518	7200	0.11	3.40	0.48	30
8	517	7300	0.11	3.00	0.63	23

[a]Using $Ru(bpy)^{3+}$ as reference with value of 0.028 in aerated water for Br and H derivatives and compound **11** in water as reference for **3**, **6**, **9** and **12**. [b]Excitation at 373 nm. [c]Determined from phosphorescence of $^1O_2$ at 1270 nm in D_2O, under air-equilibrated conditions. All solutions are isosbestic at the 532 nm excitation wavelength. [d]Triplet lifetime in Argon-saturated solution. Excitation at 532 nm.

As expected the lowest fluorescence quantum yields and the shortest lifetimes have been observed for the Br-derivatives. In fact the presence of the bromide substituent directly on the NDI core lowers both parameters due to the heavy atom effect. Concerning the tri- and tetra-derivatives we observe an unexpected effect of the length of the alkyl chain. In fact the ethyl derivatives (**1**, **3**, **7** and **9**) have better

fluorescence performance compared to the propyl derivatives (**4**, **6**, **10**, **12**). Considering the quaternary ammonium salts having all aliphatic amines positively charged and not available for eT processes one could conclude that the non-radiative deactivation processes are more efficient for compounds with the longer and more flexible alkyl spacer (n=3), as the fluorescence lifetimes are significantly reduced compared to the those of the compounds with shorter spacer (n=2, see Table 2). Indeed radiative rate constants ($k_r = \Phi/\tau$) are very similar for H and tetra-derivatives, while the rate constant for non-radiative processes of the compounds with long spacer is twice that of the compounds with shorter spacer. The fluorescence spectra of **5-7** at three different pH values are reported in ESI (Figures 4S-6S). At pH 7 we observe lower relative Φ_F values, suggesting deprotonation of an ammonium moiety and subsequent quenching of the emitting singlet excited state by intramolecular eT. The fluorescence decay is monoexponential at all pH values and the lifetimes values do not vary significantly. For a quantitative evaluation of the acidity of the ammonium moieties and the remarkable effect of the spacer length on it, fluorescence and potentiometric titrations have been performed.

Evaluation of the ground state NDIs' acidity by fluorescence and potentiometric titrations: The mode of protonation of the solubilizing amino moieties tethered to the NDI core was investigated by potentiometric and fluorescence titrations, as it controls the quenching of the excited states by eT. The NDIs **3** and **6** were chosen as model, as their fluorescence quantum yields dropped passing from pH 2 to pH 7. Fluorescence intensity change as a function of pH was analyzed for both the amines (Figure 2).

The resulting sigmoids clearly suggests that the deprotonation occurs at a lower pH for **3**. The absorption spectra of the NDIs **3** and **6** in water solutions are very similar at different pH, so the protonation state of the terminal amine groups does not influence the absorption spectra at pH $\leq$ 9. Under more basic conditions (pH$\geq$9), the amine **3** exhibited an additional absorption band at longer wavelength (λ_{max} 625 nm) than that observed under acid and neutral conditions (λ_{max} 597 nm). These

spectroscopic data suggest an aggregation of **3** in dimer and/or oligomer aggregates, rather than a deprotonation of the aromatic amine, as the latter has never been reported on similar NDIs in water. As at pH > 10 precipitation of **3** occurred, we were unable to measure its pKa_4 . Therefore, the potentiometric titration of **3** yielded only three *pKa* values*:* pKa_1 = 5.6, pKa_2 = 7.4, and pKa_3 = 7.7, suggesting that when the amine moiety is fairly close to the NDI core, due to a short alkyl spacer, the ammonium salts are rather acidic. In fact, the NDI **6** was much more basic and did not show any detectable aggregation into dimers or oligomers at pH≤12. Therefore, we were able to measure all the *pKa* constants for **6** (pKa_1 = 8.1, pKa_2 = 8.6, pKa_3 = 8.8 and pKa_3 = 11.3).

Figure 2. Fluorescence intensity (I_f) vs pH. The sigmoids defined by the (a) empty squares and (b) black circles describe the fluorescent quenching of **3** (at 640 nm) and **6** (at 661 nm), respectively, both $5x10^{-6}$M in aqueous solution, 0.1 M in $NaNO_3$.

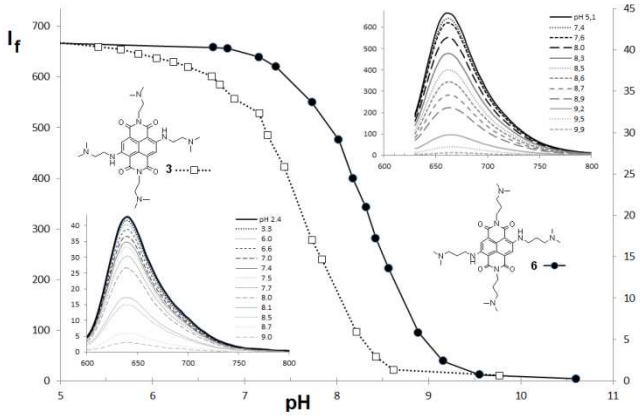

The speciation analysis in Figure 3, resulting from the potentiometric titrations describes the distribution of tetra-cationic, *vs* tri-, bis-, mono-cationic and neutral NDIs (NDI-H_4, NDI-H_3, NDI-H_2, NDI-H and NDI, respectively) as function of the pH. These data suggest that the amine **6** is mainly fully protonated at pH 7 (94% of **6**-H_4), unlike the amine **3**, which exists as a mixture of both tri- (68%, **3**-H_3) and di-cationic (26%, **3**-H_2) species.

Figure 3. Speciation analysis resulting from the potentiometric titrations for the NDIs (a) **3** (tetr-cationic **3**-H_4, tri-cationic **3**-H_3, and di-cationic **3**-H_2 distribution is reported) and (b) **6** (the distribution of **6**-H_4, **6**-H_3, **6**-H_2, **6**-H and **6** are reported). The diamonds describe the fluorescent quenching.

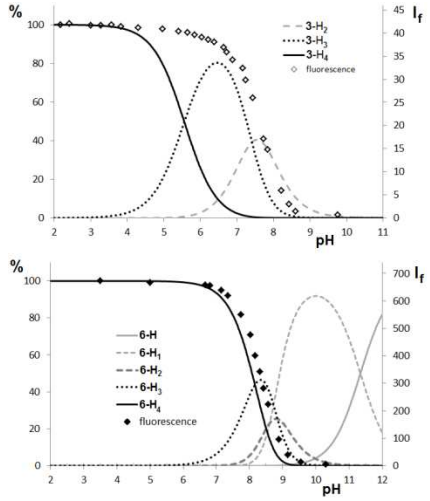

These data clearly indicate the NDI **6** is a better fluorescent probe than **3** under physiological conditions; being fully protonated, it is not quenched by intra-molecular eT. Surprisingly, the fluorescence quenching of **3** occurs during the deprotonation of the second ammonium moiety in the specie **3**-H_3, probably because the first free amino group is not enough electron donor due to the closer NDI core. On the contrary, the fluorescence quenching of **6** follows the deprotonation of the tetracationic specie **6**-H_4.

Spectroscopic and Kinetic Characterization of the NDI Triplet State: To provide a full characterization of the synthesized NDI as singlet oxygen sensitizers, it is mandatory to examine the key features of their triplet states. In fact, both the population of the triplet excited states and their lifetimes have a direct effect on the efficiency for singlet oxygen production. Therefore, we set out to examine these issues in detail for several of our NDIs, in acetonitrile and in water solution under neutral and slightly acidic conditions (pH 5 and 7), by nanosecond laser flash photolysis using a Nd-YAG laser, operating at both 532 and 355 nm. Upon laser excitation at both 355 and 532 nm, transient absorption spectra in the range of 380-750 nm, with λ_{max} at 430 nm, were observed for all the substituted NDIs

investigated. A second broad band exhibiting λ_{max} centered at 530, 630 and 670-690 nm was recorded for the mono-substituted (**1** and **4**), Br-substituted (**2** and **5**), and NHR di-substituted NDIs (**9** and **12**) (Figures 4 and 5).

Figure 4. Time-resolved difference absorption spectra flashing a $8x10^{-6}$M solution of **1**, **2** (at 355 nm), **3** (at pH 5) and **9** (at pH 7), both at 532 nm, in argon purged 10^{-2} M phosphate buffer.

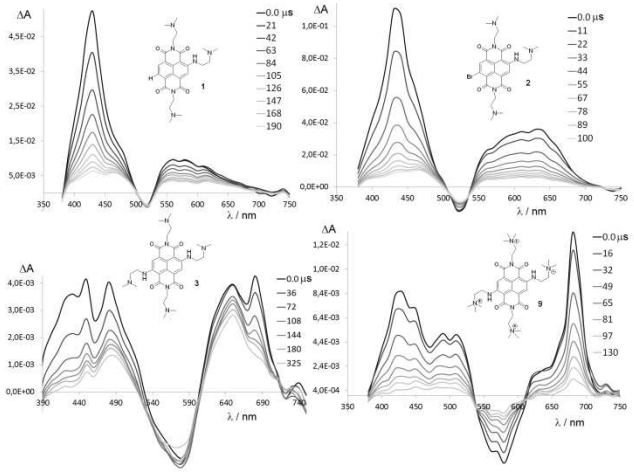

Figure 5. Time-resolved difference absorption spectra flashing a $8x10^{-6}$M solution of **4**, **5** (at 355 nm), **6** (at pH 5) and **12** (at pH 7), both at 532 nm, in argon purged 10^{-2} M phosphate buffer.

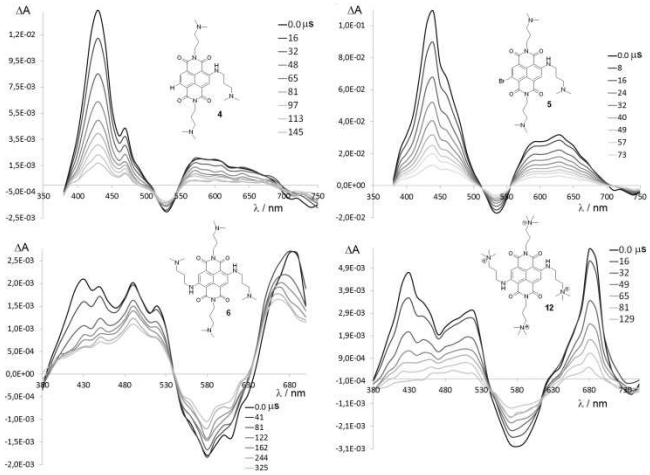

Likely the electron donor character of the second substituent on the NDI core, passing from H, Br to

NHR, resulted in a progressive red shift of the second band, which also became more intense. Bleaching at 510-550 nm and 550-600 nm for the NDIs **1**, **2**, **4**, **5** and **3**, **6**, **9**, **12**, respectively was due to the depletion of the ground state of the NDIs upon excitation to the triplet excited state. All transient absorption profiles monitored at both 430 nm and 680 nm decay monoexponentially in air-equilibrated solutions with a lifetime of ~ 2 μs (Figure 6).

In argon-saturated solutions lifetimes increase to ca. 20-30 μs, indicating that at pulse end we are very likely observing the triplet state absorption. The transient absorption spectra in Ar-saturated solution observed from the pulse end to 80 μs after (Figures 3 and 4) have been assigned to the triplet state of each NDI, on the basis of its sensitivity to O_2 and similarity to the T_1-T_n absorption of non-water soluble NDIs.[34] The amines **3** and **6** exhibit a fairly similar spectra at pulse end to their quaternary ammonium analogues **9** and **12**. Nevertheless, at pH 5 both the amines **3**, and **6** reveal also the generation of a more stable species on a longer time scale (>200 μs). This second species, which was completely bleached by oxygen also exhibits an absorption spectra (λ_{max} 480-490 nm and 660 nm) fairly similar to the stable species generated by NDI mono-electronic reduction. Therefore it can be assigned to the NDI radical anions $\mathbf{3}^{\bullet-}$ and $\mathbf{6}^{\bullet-}$ generated by eT from free amine to the excited NDI core.[35-37] In the hypothesis that the NDIs **3** and **9** and the homologues **6** and **12** have similar molar absorption coefficients for T-T absorption at 430 nm, we see that initial absorbance is much higher for **12** compared to the other tetra-substituted compounds **3**, **6** and **9** (Figure 6). This allows us to conclude that the triplet is likely formed with much higher efficiency in the case of **12**. It is somewhat surprising that its analogue **6** at pH 2 did not efficiently produce the triplet excited state. In spite of very similar fluorescence properties of **6** and **12** the triplet formation yield seems much lower. A possible explanation for this behavior may be the presence of the carbonyl group enabling excited state intramolecular proton transfer (ESIPT) from the protonated aliphatic amine to the carbonyl.[38]

Figure 6. Differential absorption decay monitored at a) 430 nm and b) 660 nm for **3**, **6**, **9**, and **12** ($8x10^{-5}$M) and c) 430 nm for **2**, **5**, **8**, and **11** ($4x10^{-5}$M), in air equilibrated neutral D_2O solution (**9**, **12**, **8** and **11**) or acidic D_2O of pH 2 (**3**, **6**, **2**, and **5**). All the solution were excited at 532 nm where they exhibited identical absorbance of 0.3.

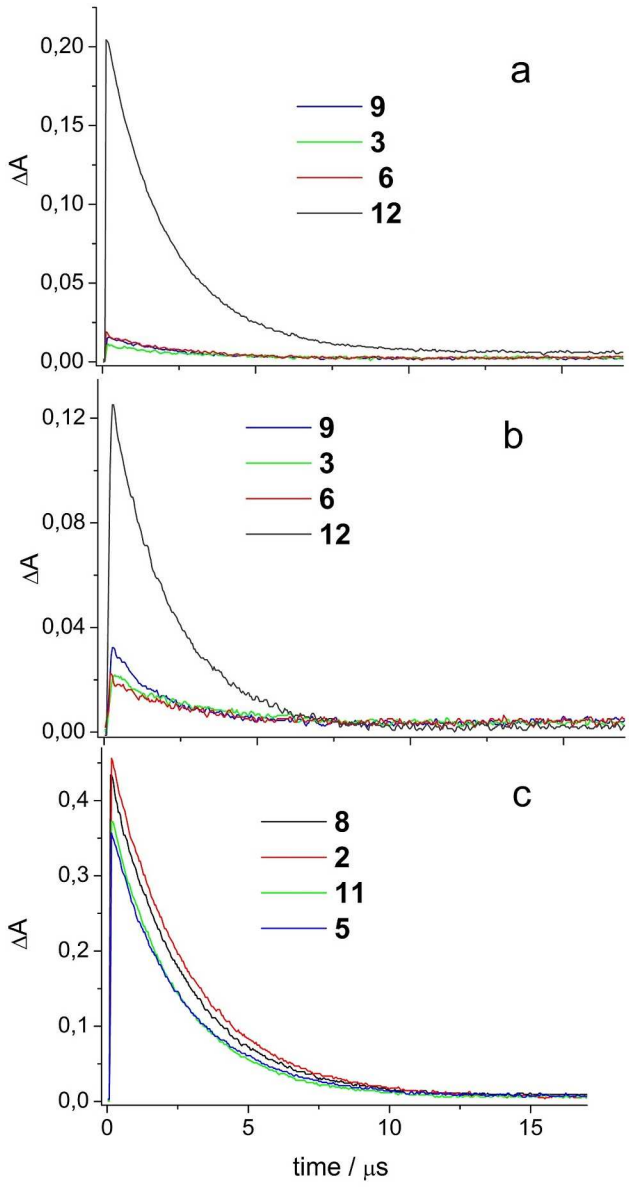

Singlet Oxygen Generation Efficiency: The fluorescence data are coherent with the ability of singlet oxygen production of these compounds. The singlet oxygen quantum yields (Φ_Δ) reported in the present study, and listed in Table 2, were obtained in time-resolved experiments by comparing the initial intensity of the 1270 nm singlet oxygen phosphorescence decay (Figure 7) produced upon irradiation at

532 nm, (by means of a Nd-YAG laser) of the given NDIs, to that of 5,10,15,20-tetrakis(4-sulfonatophenyl) porphyrin (TPPS) as standard sensitizer (Φ_Δ=0.76).[39,40]

As expected the Br-derivatives (**2**, **5**, **8** and **11**) produce $^1O_2$ in water. Our approach to introduce a Br substituent favoring intersystem crossing gave thus positive results. The Φ_Δ values are good ranging from 0.39 to 0.63, even though they are lower compared to the TPPS value. From the point of view of application in PDT their absorption extending up to 550 nm represents, however, a drawback. Under the very same experimental conditions the Br-derivatives exhibit higher Φ_Δ than that of the another conventional photosensitizer Rose Bengal (Figure 7). Such a difference may be due to aggregation and T-T annihilation known to occur for Rose Bengal.

Figure 7. Time-resolved phosphorescence signal of singlet oxygen in D_2O (monitored at 1270 nm), using the standards TPPS and Rose Bengal and the NDIs **2**, **3**, **5**, **8**, **9**, **11**, **12** as photosensitizers. For the amines **2**, **3** and **5** the pH was set to 2, by DCl addition. Excitation with Nd-YAG laser at 532nm; energy of 3.6 mJ/pulse; all solutions absorb equally at 532 nm.

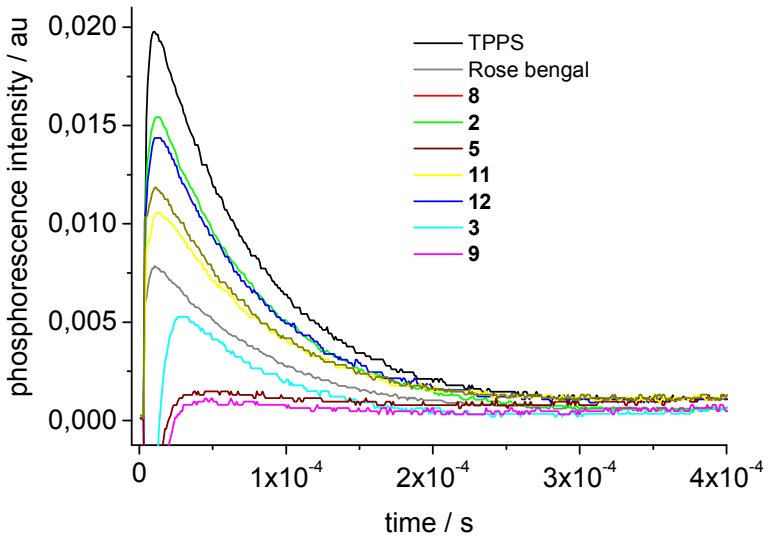

More surprisingly, the quaternary ammonium salt **12** was the only NDI among those without Br, able

to produce singlet oxygen in water with a very satisfactory yield (0.30). Such an efficiency was even more striking in comparison to the very low Φ_Δ (0.07) for its analogue **9**, exhibiting a shorter alkyl spacer (n=2). The related ethyl- (n=2) and propyl- (n=3) amino analogues **3** and **6**, produce singlet oxygen with negligible yields (≤0.04), even at pH 2, which ensuring complete protonation of all the amino moieties, erased the excited state quenching by intramolecular eT. As suggested above this behavior may be due to the presence of the carbonyl group enabling excited state intramolecular proton transfer from the protonated aliphatic amine to the carbonyl.[38] This however does not explain the poor behavior of compound **9** with respect to that of **12**.

Photooxidation of 1,5-dihydroxynaphthalene and 9,10-anthracenedipropionic acid in acetonitrile and water by the tetra-cationic NDI 12. Sensitizers such as **12**, which are characterized by (i) intense absorption of red visible light, (ii) long living triplet and (iii) high singlet oxygen yields are ideal for performing efficient photo-oxidations. In addition, the solubility of **12** in both acetonitrile, and water allows to exploit its properties as singlet oxygen sensitizer in both solvents, also targeting water soluble biomolecules. Thus, as a proof of concept, we decided to investigate **12** as singlet oxygen sensitizer in the photo-oxidation of 1,5-dihydroxynaphthalene (DHN) and 9,10-anthracenedipropionic acid (ADPA) in acetonitrile and water, respectively. Visible light at longer wavelength than 500 nm was used. DHN was efficiently oxidized to its naphthoquinone derivative (5-hydroxy-1,4-naphthalenedione) through the endo-peroxide, by $^1O_2$.[41] The resulting naphthoquinone absorbing at 360-440 nm, has been efficiently monitored by the increase of its absorption, which appeared to be in the spectroscopic window where the NDI shows negligible absorption (Figure 8a).

Unfortunately, the solubility in water of DHN is very poor, and we were able to perform a photo-oxidation of DHN only in aqueous acetonitrile (Supp. Inf.). Therefore, DHN has been replaced by ADPA as water soluble $^1O_2$ trap.[42] Contrary to DHN, in this case, the photo-oxidation has been followed by the decrease absorption at 400 nm due to the consumption of ADPA anthracene chromophore, forming a colorless endo-peroxide (Figure 8b). Continuous photobleaching of the anthracene absorption

was observed for 10 h by using excitation wavelength longer than 450 nm. Byproduct formation was not detected by UV-absorption during the irradiation. No decrease in the anthracene absorbance was observed in the solutions without the sensitizer. To our knowledge this is the first fairly efficient photo-bleaching experiments of ADPA, performed in H_2O, rather than in D_2O, where the lifetime of singlet oxygen is much longer. This evidence further suggests that **12** is a promising singlet oxygen sensitizer for biological applications. A small blue shift (6 nm) of the absorption at 640 nm was detected during the photooxidation, suggesting a weak interaction between ADPA and the NDI core, in water solution.

Figure 8. Change in the absorption spectra by irradiation (at $\lambda > 450$nm) of (a) an acetonitrile solution of DHN ($1.2x10^{-4}$ M) and (b) an aqueous solution of ADPA ($1.2x10^{-4}$ M), using **12** ($2x10^{-5}$M and $6x10^{-5}$ M, respectively) as singlet oxygen photosensitizer.

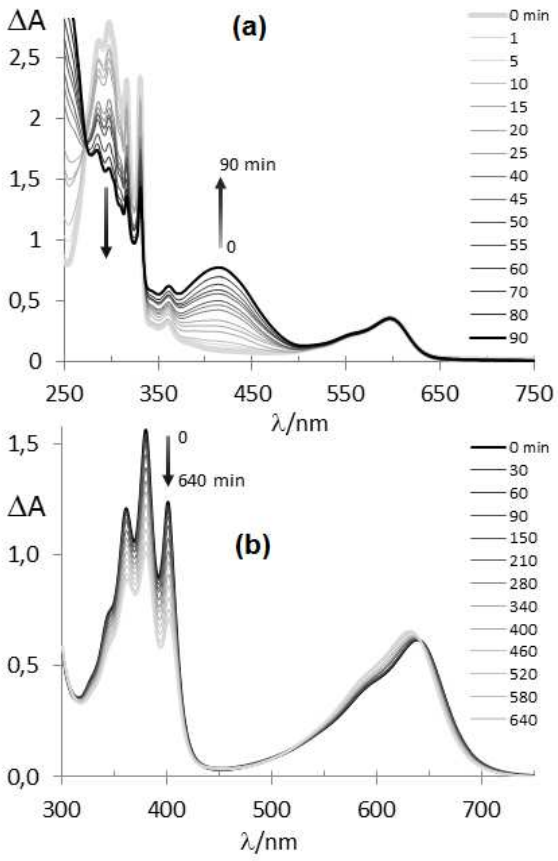

Conclusions

Naphthalene diimide derivatives with bromo and amino or quaternary ammonium substituents on both the aromatic core and the imide moieties were prepared as water soluble singlet oxygen sensitizers, in which water solubility derived from ionic substituents. Their photophysical properties were thoroughly investigated by steady-state and time-resolved spectroscopy. The red colored Br-containing NDIs (**2**, **5**, **8** and **11**) were very efficient singlet oxygen sensitizers in water solution. Unfortunately their absorbing wavelength was centered at 537 nm, slightly below the PDT spectroscopic window. On the contrary, the blue colored tetra-cationic NDI **12** retains a comparable efficiency in the generation of $^1O_2$, coupled to an absorption in the red. Moreover, all the NDI investigated, including the best singlet oxygen sensitizers, also exhibited a remarkable red (for the Br-NDIs **2**, **5**, **8** and **11**) and NIR (tetra-substituted NDIs **3**, **6**, **9** and **12**) fluorescence emission with lifetimes that are longer than those of intrinsic biological fluorophores. These evidences make them very appealing candidates for multimodal applications as fluorescent reporters and efficient photosensitizers for PDT. Moreover, taking into consideration that cationic NDIs have already been proved to be excellent and selective G-quadruplex ligands, NDIs such as **12** may be exploited as selective G4 ligand as well as agent to achieve photocleavage footprinting of G-quadruplex folding nucleic acids. These aspects are currently under investigation.

Experimental Section

Synthesis and Purification. The NDIs **1**, **3**, **4** and **6** have been already synthesized and characterized.[14] In this study they have been synthesized following a more efficient protocol, starting from the precursors **14** and **15**. The anhydride **13** and the NDIs **14**, **15** have been synthesized according to published procedures.[17,19] HPLC analysis and purifications were performed using both preparative and analytical HPLCs. The analytical column was XSelect CSH Phenyl-Hexyl (150 x 4.6 mm). The preparative column was XSelect CSH Prep Phenyl-Hexyl 5μm (150 x 30 mm). Flows were 1 ml/min for

analytical and 27 ml/min for preparative. An analytical method was used: method A (Aqueous solvent: 0.1% trifluoroacetic acid in water; organic solvent: Acetonitrile; Gradient: 95% aqueous, gradually to 0% aqueous over 14 minutes and at the end an isocratic flow over 2 minutes). Preparative HPLC were performed using method B (Aqueous solvent: 0.1% trifluoroacetic acid in water; organic solvent: Acetonitrile; Gradient: 95% aqueous, gradually to 20% aqueous over 18 minutes and at the end an isocratic flow over 4 minutes). ^{1}H-, ^{13}C-NMR spectra were recorded on a 300 MHz spectrometer and the chemical shifts are reported relative to TMS. The structures of new compounds were deduced from the results of ^{1}H-, and ^{13}C-NMR.

Nucleophilic aromatic substitution reaction at r.t., optimized for Br-NDI synthesis. The NDI **14-15** (0.5 mmol) was dissolved into 40 ml of acetonitrile in a round bottom flask together with the corresponding amine (N,N-dimethyl-ethylamine for **1-2** and N,N-dimethyl-propylamine for **4-5**; 1.5 mmol). The mixture was stirred at 70°C for 4 h under argon. The resulting red solution was concentrated under vacuum and a red solid was obtained. The crude product was purified by preparative HPLC chromatography, using a C-18 reverse phase column, (CH_3CN:H_2O 0.1%TFA) according to analytical method B. HCl 1 M solution was added to each chromatographic portion. Solvent evaporation under vacuum at r.t. afforded the adducts **1** (99.4 mg, 33% yield), **2** (142.8 mg, 42%), **4** (93.7 mg, 29%), and **5** (163.1 mg, 45%) as hydrochlorides.

***N,N*'-Bis-((dimethylamino)ethylamino)-2-bromo-6-((dimethylamino)ethylamino)-1,4-5,8-naphthalenetetracarboxylic bisimide trihydrochloride** (**2**·3HCl): The collected solid was purified by preparative HPLC chromatography (CH_3CN:H_2O 0.1%TFA). Red solid; m.p. dec.>350°C. ^{1}H-NMR (300 MHz, D_2O): 8.68 (s, 1H), 8.3 (s, 1H), 4.74 (m, 4H), 4.38 (m, 2H), 3.96 (m, 2H), 3.75 (m, 4H), 3.41 (bs, 18H). ^{13}C-NMR (75 MHz, D_2O): 165.1; 162.3; 161.6; 151.1; 137.6; 127.9; 126.7; 122.7; 121.1; 120.8, 120.4; 100.7; 64.1; 62.0; 61.7; 53.6; 53.3; 36.9; 34.7; 34.0. Anal. Calcd. for $C_{26}H_{36}BrCl_3N_6O_4$: C, 45.73; H, 5.31; N, 12.31. Found: C, 45.82; H, 5.29; N, 12.24.

***N,N'*-Bis-((dimethylamino)propylamino)-2-bromo-6-((dimethylamino) propylamino)-1,4-5,8-naphthalenetetracarboxylic bisimide trihydrochloride** (**5**·3HCl): The collected solid was purified by preparative HPLC chromatography (CH_3CN:H_2O 0.1%TFA). Red solid; m.p. dec.>350°C. ^{1}H-NMR (300 MHz, CD_3OD): 8.21 (s, 1H); 8.00 (s, 1H); 4.15 (m, 4H); 3.76 (t, ^3J=7.6 Hz, 2H); 3.43 (m, 2H); 3.31 (m. 4H); 3.27 (s, 6H); 2.94 (s, 12H); 2.34 (m, 2H); 2.17 (m, 4H). ^{13}C-NMR (75 MHz, CD_3OD): 166.8; 163.1; 162.4; 152.8; 138.4; 129.3; 128.3; 124.1; 123.9; 122.3; 121.5; 121.2, 101.0; 57.0; 56.9; 56.7; 43.8; 41.4; 39.5; 38.8; 26.1; 24.8; 24.7. Anal. Calcd. for $C_{29}H_{42}BrCl_3N_6O_4$: C, 48.05; H, 5.84; N, 11.59. Found: C, 47.95; H, 5.82; N, 11.66.

General procedure for the Microwave assisted (MW) nucleophilic aromatic substitution, optimized for NDIs containing no Br. The NDI **14-15** (0.5 mmol) was dissolved into 6 ml of dry DMF in MW-vial together with the corresponding amine (N,N-dimethyl-ethylamine for **3** and N,N-dimethyl-propylamine for **6**; 1.5 mmol). The mixture was stirred and heated in a microwave reactor, according a closed vessel protocol, at 135 °C, 200 psi, 200 W, for 3 min. The resulting dark-violet solution was cooled at r.t. and water (50 ml) was added to induce precipitation. The filtered crude product was purified by preparative HPLC chromatography, using a C-18 reverse phase column (CH_3CN:H_2O 0.1%TFA, method B). HCl 1 M solution was added to each chromatographic portion. Solvent evaporation under vacuum afforded the adducts **1 1** (152.5 mg, 51%, yield), **3** (97.8, 27%) and **4** (148.6 mg, 46%), **6** (125.2 mg, 32%) as hydrochlorides.

Exhaustive methylation of the NDI 1-5. The NDIs purified as hydrochlorides were dissolved in a $NaHCO_3$ solution and extracted 3 times with CH_2Cl_2. The recovered organic layers have been dried on Na_2SO_4 and the solvent evaporated under reduced pressure. The collected amine (0.5 mmol) was suspended in 50 ml of CH_3CN and 0.24 g (1.7 mmol) of CH_3I were added. This suspension was stirred under nitrogen atmosphere for 12 h. After this period the solvent was removed under vacuum, and the crude was purified by preparative HPLC, using a C-18 reverse phase column (CH_3CN:H_2O 0.1%TFA,

method B). HCl 1 M solution was added to each chromatographic portion. Solvent evaporation under vacuum at r.t. afforded the adducts to give the quaternary ammonium salts as chlorides **7-11**.

***N,N'*-Bis-((trimethylamino)ethylamino)-2-((trimethylamino)ethylamino) -1,4-5,8-naphthalene tetracarboxylic bisimide trichloride** (**7**): Red solid, 309 mg, yield 96%; m.p.>350°C. ^{1}H-NMR (300 MHz, D_2O): 8.59 (d, ^{3}J=7.9 Hz, 1H); 8.33 (d, ^{3}J=7.9 Hz, 1H); 8.24 (s, 1H); 4.63 (m, 4H); 4.27 (t, ^{3}J=6.5 Hz, 2H); 3.84 (t, ^{3}J=6.5 Hz, 2H); 3.71 (m, 4H); 3.31 (s, 27H). ^{13}C-NMR (75 MHz, D_2O): 165.7; 164.3; 164.1; 163.7; 151.8; 131.5; 129.2; 127.9; 125.9; 125.2; 123.2; 119.8; 118.7, 101.0; 64.2; 62.3; 62.0; 53.7; 53.3; 36.8; 34.3; 33.9. Anal. Calcd. for $C_{29}H_{43}Cl_3N_6O_4$: C, 53.91; H, 6.71; N, 13.01. Found: C, 54.03; H, 6.70; N, 13.11.

***N,N'*-Bis-((trimethylamino)ethylamino)-2-bromo-6-((trimethylamino)ethylamino) -1,4-5,8-naphthalenetetracarboxylic bisimide trichloride** (**8**): Red solid, 325 mg, yield 90%; m.p.>350°C. ^{1}H-NMR (300 MHz, D_2O): 8.53 (s, 1H); 8.19 (s, 1H); 4.59 (m, 4H); 4.25 (t, ^{3}J=6.3 Hz, 2H); 3.84 (t, ^{3}J=6.3 Hz, 2H); 3.62 (m, 4H); 3.29 (s, 27H). ^{13}C-NMR (75 MHz, D_2O): 165.0; 162.2; 161.6; 151.0; 137.5; 127.9; 126.7; 122.6; 121.1; 120.8; 120.3; 100.6; 63.9; 61.8; 61.6; 53.5; 53.2; 36.8; 34.6; 33.9. Anal. Calcd. for $C_{29}H_{42}BrCl_3N_6O_4$: C, 48.05; H, 5.84; N, 11.59. Found: C, 48.22; H, 5.78; N, 11.35.

***N,N'*-Bis-((trimethylamino)ethylamino)-2,6-((trimethylamino)ethylamino) -1,4-5,8-naphthalenetetracarboxylic bisimide tetrachloride** (**9**): Violet solid, 386 mg, yield 99%; m.p.>350°C. ^{1}H-NMR (300 MHz, D_2O): 8.10 (s, 2H); 4.59 (m, 4H); 4.11 (m, 4H); 3.71 (m, 4H); 3.59 (m, 4H); 3.21 (s, 36H). ^{13}C-NMR (75 MHz, D_2O): 167.4; 165.4; 164.6; 164.1; 150.0; 127.2; 123.1; 119.7; 115.9; 104.6; 65.7; 63.7; 55.0; 54.8; 38.0; 35.4. Anal. Calcd. for $C_{34}H_{56}Cl_4N_8O_4$: C, 52.18; H, 7.21; N, 14.32. Found: 52.31; H, 7.18; N, 14.27.

***N,N'*-Bis-((trimethylamino)propylamino)-2-((trimethylamino)propylamino)-1,4-5,8-naphthalenetetracarboxylic bisimide trichloride** (**10**): Red solid, 337 mg, yield 98%; m.p.>350°C. ^{1}H-NMR (300 MHz, D_2O): 8.2 (d, ^{3}J=7.9 Hz, 1H); 7.97 (d, ^{3}J=7.9 Hz, 1H); 7.79 (s, 1H); 4.11 (m, 4H);

3.68 (t, 2H); 3.46 (m, 6H), 3.10 (s, 9H); 3.06 (s, 18H); 2.16 (m, 6H). ^{13}C-NMR (75 MHz, D_2O): δ=165.3; 163.8; 163.6; 163.3; 151.7; 130.8; 128.6; 127.0; 125.1; 124.4; 122.3; 119.6; 118.6, 99.5; 63.9; 52.9; 39.5; 37.7; 37.1; 22.9; 21.4. Anal. Calcd. for $C_{32}H_{49}Cl_3N_6O_4$: C, 55.85; H, 7.18; N, 12.21. Found: C, 55.71; H, 7.27; N, 12.30.

***N,N*'-Bis-((trimethylamino)propylamino)-2-bromo-6-((trimethylamino) propylamino)-1,4-5,8-naphthalenetetracarboxylic bisimide trichloride** (**11**): Red solid, 372 mg, yield 97%, m.p.>350°C. ^{1}H-NMR (300 MHz, D_2O): 8.18 (s, 1H); 7.92 (s, 1H); 4.05 (m, 4H); 3.68 (m, 2H); 3.49 (m, 2H); 3.38 (m, 4H), 3.10 (s, 9H); 3.03 (s, 18H); 2.24 (m, 2H); 2.10 (m, 4H). ^{13}C-NMR (75 MHz, D_2O): 165.0; 162.2; 162.0; 161.3; 151.2; 137.0; 127.5; 126.1; 121.9; 120.4; 119.9; 118.0; 114.1, 99.2; 63.8; 52.8; 39.6; 38.1; 37.2; 22.7; 21.2; 21.1. Anal. Calcd. for $C_{32}H_{48}BrCl_3N_6O_4$: C, 50.11; H, 6.31; N, 10.96. Found: C, 49.89; H, 6.35; N, 11.03.

General protocol for exhaustive methylation of tetra-substituted-NDI 6: The NDI **6** purified as hydrochloride was dissolved in a Na_2CO_3 solution and extracted 3 times with CH_2Cl_2. The recovered organic layers have been dried on Na_2SO_4 and the solvent evaporated under reduced pressure. The collected amine (0.5 mmol) was added to a suspension of Na_2CO_3 (2 mmol) in 50 ml of CH_3CN and 0.24 g (1.7 mmol) of CH_3I were added. This suspension was stirred under nitrogen atmosphere for 12 h. After this period the solvent was removed under vacuum to give the and the crude was purified by preparative HPLC, using a C-18 reverse phase column (CH_3CN:H_2O 0.1%TFA, method B). HCl 1 M solution was added to each chromatographic portion. Solvent evaporation under vacuum at r.t. afforded the adducts to give the quaternary ammonium salt as chloride **12** (415 mg, 99%, yield).

***N,N*'-Bis-((trimethylamino)propylamino)-2,6- ((trimethylamino)propylamino) -1,4-5,8-naphthalenetetracarboxylic bisimide tetrachloride** (**12**): Violet-dark solid, yield 99%; m.p.>350°C. ^{1}H-NMR (300 MHz, D_2O): 7.62 (s, 2H); 4.14 (m, 4H); 3.62 (m, 4H); 3.49 (m, 8H); 3.08 (s, 18H); 3.06 (s, 18H); 2.17 (m, 8H). ^{13}C-NMR (75 MHz, D_2O): 165.3; 163.3; 148.2; 124.6; 120.5; 117.3, 101.6;

64.1; 53.1; 39.2; 37.3; 22.7; 21.6. Anal. Calcd. for $C_{38}H_{64}Cl_4N_8O_4$: C, 54.41; H, 7.69; N, 13.36. Found: C, 54.22; H, 7.79; N, 13.26.

Sample Preparation for Solution Studies. For the spectroscopic measurements we used pure water as well as 10 mM K^+ phosphate buffer of pH 2 adjusted with aliquots of HCl 3N.

Absorption and fluorescence spectra. UV-visible absorption spectra were recorded on a standard commercial spectrophotometer. Fluorescence spectra were measured using 1 nm steps and 0.5 s dwell time. Slits were kept narrow to 1 nm in excitation and 1 or 2 nm in emission. Where necessary a cut-off filter was used. Right angle detection was used. All the measurements were carried out at 295 K in quartz cuvettes with path length of 1 cm. All fluorescence spectra have been obtained for air-equilibrated solutions absorbing less than 0.1 at all wavelengths to avoid inner filter effects and re-absorption of emission. Furthermore, they have been corrected for wavelength dependent response of the monochromator/PMT couple. The compound $Ru(bpy)_3Cl_3.xH_2O$ dissolved in air-equilibrated water with known fluorescence quantum yield (Φ_F) of 0.028 was used as standard for the determination of the fluorescence quantum yield of the NDI samples. The Φ_F value obtained for the compound **11** in water was used as reference to determine the fluorescence quantum yield of the tetra-NDI compounds (**3**, **6, 9** and **12**), excited at 546 nm. Using the same solvents for all compounds and iso-absorbing solutions at the excitation wavelength no corrections had to be made for absorbance neither solvent refraction index and we calculated the fluorescence quantum yields, Φ_F, using the formula below, with A being the integrated area of the corrected fluorescence spectra:

$$\Phi_F = \Phi_F^{ref} \times A/A^{ref} \qquad (1)$$

Fluorescence lifetimes. They were measured in air-equilibrated solutions with a time correlated single photon counting system. A nanosecond LED source at 373 nm was used for excitation and the emission was collected at right angle at 580 nm or 635 nm using a long pass cut-off filter at 495 nm.

Decay profiles were fitted using a mono- or multiexponential function and deconvolution of the instrumental response.

$$I(t) = \sum_i a_i \times \exp(-t/\tau_i) \quad (2)$$

$$f_i = (a_i \times t_i)/ \sum_j (a_j \times t_j) \quad (3)$$

Nanosecond laser flash photolysis. The pulse of a Nd-YAG laser, operating at 355 and 532 nm (20 ns FWHM, 2 Hz), was suitably shaped passing through a 3 mm high and 10 mm wide rectangular window, and providing a fairly uniform energy density of 2.7 mJ/pulse corresponding to 9 mJ/cm^2 incident on the sample cell. A front portion of 2 mm of the excited solution was probed at right angle, the useful optical path for analyzing light being 10 mm. A_{532} was ~ 0.3 over 1 cm. Ar-saturated or air-equilibrated solutions were used. The sample was renewed after few laser shots. Temperature was 295 K.

Singlet oxygen time resolved emission measurements. The pulse of a Nd-YAG laser, operating at 532 nm (20 ns FWHM, 2 Hz), was used for excitation of the reference TPPS and the NDI samples dissolved in air-equilibrated deuterated water. We used DCl to adjust pH values to 2 when necessary. All solutions had identical absorbance of ca. 0.3 at the 532 nm excitation wavelength. A preamplified (low impedance) Ge-photodiode cooled at 77 K (Applied Detector Corporation, Model 403HS, time resolution 300 ns) and equipped with a 5 mm thick AR coated silicon metal filter with wavelength pass >1.1 μm and an interference filter at 1.27 μm was used to measure emission of singlet oxygen at 1270 nm in right angle geometry. The photodiode output current was fed into a digital oscilloscope. The intensities of singlet oxygen emission of reference and sample can be compared directly with each other and the calculation of the singlet oxygen emission quantum yield, Φ_Δ, is based on the following equation:

$$\Phi_{\Delta} = \Phi_{\Delta}^{ref} \times I_0/I_0^{ref} \quad (4)$$

where I_0 is the emission intensity extrapolated at time zero upon single exponential fitting of the emission decay with the exclusion of the initial part of the signal affected by scattered light, sensitizer fluorescence and formation kinetics. The standard value of 0.76 was used for Φ_{Δ}^{ref} of TPPS.[40]

Fluorescence Quenching and Potentiometric titrations. Spectrofluorimetric were performed with on a commercial spectrophotometer. The pH-metric titrations were carried out with a commercial titration system. All titrations were performed at 25.0 ± 0.1 °C. Protonation constants of ligand L were determined in a water mixture, made 0.1 M in $NaNO_3$. In a typical experiment, 15 mL of a 5×10^{-4} M ligand solution were treated with an excess of a 1.0 M HNO_3 standard solution. Titrations were run by addition of 10 μL aliquots of carbonate-free standard 0.1 M NaOH, recording 80-100 points for each titration. Prior to each potentiometric titration, the standard electrochemical potential (E°) of the glass electrode was determined in the water, by a titration experiment according to the Gran method.[43] Protonation titration data (emf *vs.* mL of NaOH) were processed with the Hyperquad package,[44] to determine the equilibrium constants.

Associated Content

Supporting Information. Additional Absorption and Fluorescence spectra (Figure 1-6S), Time-correlated single photon counting experiments (TCSPC, Figure 7S), HPLC purity data and NMR spectra of the new NDIs. This material is available free of charge via the Internet at http://pubs.acs.org

Author information

*Corresponding Author. Fax: +39 0382 987323. Tel: +39 0382 987668. E-mail:

mauro.freccero@unipv.it

Notes

The authors declare no competing financial interest.

Acknowledgements

Financial support from MIUR, Rome (FIRB-IdeasRBID082ATK, and PRIN 2009MFRKZ8), and University of Pavia, is gratefully acknowledged. I.M. likes to thank Dr. F. Manoli for assistance in practical laboratory issues.

References

(1) Brown, S. B.; Brown, E. A.; Walker, I. *Lancet Oncol.* **2004**, *5*, 497-508.
(2) Jiang, X. J.; Lo, P. C.; Tsang, Y. M.; Yeung, S. L.; Fong, W. P.; Ng, D. K. *Chem.-Eur. J.* **2010**, *16*, 4777-4783.
(3) Lo, P. C.; Huang, J. D.; Cheng, D. Y.; Chan, E. Y.; Fong, W. P.; Ko, W. H.; Ng, D. K. *Chem. Eur. J.* **2004**, *10*, 4831-4838.
(4) Schweitzer, C.; Schmidt, R. *Chem. Rev.* **2003**, *103*, 1685-1757.
(5) Stefflova, K.; Chen, J.; Zheng, G. *Curr. Med. Chem.* **2007***, 14,* 2110-2125.
(6) Barker, C. A.; Zeng, X. S.; Bettington, S.; Batsanov, A. S.; Bryce, M. R.; Beeby, A. *Chem. Eur. J.* **2007***, 13,* 6710-6717.
(7) Ishii, K. *Coord. Chem. Rev.* ***2012****, 256,* 1556-1568.
(8) Jiang, X. J.; Yeung, S. L.; Lo, P. C.; Fong, W. P.; Ng, D. K. *J. Med. Chem.* **2011***, 54,* 320-330.
(9) Strassert, C. A.; Otter, M.; Albuquerque, R. Q.; Hone, A.; Vida, Y.; Maier, B.; De Cola, L. *Angew. Chem. Int. Ed. Engl.* **2009***, 48,* 7928-7931.
(10) Tu, J.; Wang, T. X.; Shi, W.; Wu, G. S.; Tian, X. H.; Wang, Y. H.; Ge, D. T.; Ren, L. *Biomaterials* **2012**, *33*, 7903-7914.
(11) Wu, W.; Guo, H.; Wu, W.; Ji, S.; Zhao, J. *J. Org. Chem.* **2011***, 76,* 7056-7064.
(12) Sakai, N.; Mareda, J.; Vauthey, E.; Matile S. *Chem. Commun.,* **2010**, *46*, 4225–4237.
(13) Collie, G. W.; Promontorio, R.; Hampel, S. M.; Micco, M.; Neidle, S.; Parkinson, G. N. *J. Am. Chem. Soc.* **2012***, 134,* 2723-2731.
(14) Cuenca, F.; Greciano, O.; Gunaratnam, M.; Haider, S.; Munnur, D.; Nanjunda, R.; Wilson, W. D.; Neidle, S. *Bioorg. Med. Chem. Lett.* **2008**, *18*, 1668-1673.

(15) Micco, M.; Collie, G. W.; Dale, A. G.; Ohnmacht, S. A.; Pazitna, I.; Gunaratnam, M.; Reszka, A. P.; Neidle, S. *J. Med. Chem.* **2013**, *56*, 2959-2974.

(16) Di Antonio, M.; Doria, F.; Richter, S. N.; Bertipaglia, C.; Mella, M.; Sissi, C.; Palumbo, M.; Freccero, M. M. Di Antonio, F. Doria, S. N. Richter, C. Bertipaglia, M. Mella, C. Sissi, M. Palumbo, M. Freccero, *J. Am. Chem. Soc.* **2009**, *131*, 13132-13141.

(17) Doria, F.; Nadai, M.; Folini, M.; Di Antonio, M.; Germani, L.; Percivalle, C.; Sissi, C.; Zaffaroni, N.; Alcaro, S.; Artese, A.; Richter, S. N.; Freccero, M. *Org. Biomol. Chem.* **2012**, *10*, 2798-2806.

(18) Doria, F.; Nadai, M.; Folini, M.; Scalabrin, M.; Germani, L.; Sattin, G.; Mella, M.; Palumbo, M.; Zaffaroni, N.; Fabris, D.; Freccero, M.; Richter, S. N. *Chem.-Eur. J.* **2013**, *19*, 78-81.

(19) Nadai, M.; Doria, F.; Di Antonio, M.; Sattin, G.; Germani, L.; Percivalle, C.; Palumbo, M.; Richter, S. N.; Freccero, M. *Biochimie* **2011**, *93*, 1328-1340.

(20) Siddiqui-Jain, A.; Grand, C. L.; Bearss, D. J.; Hurley, L. H. *Proc. Natl. Acad. Sci. USA,* **2002**, *99*, 11593-11598.

(21) Huppert, J. L.; Balasubramanian, S. *Nucleic Acids Res.* **2005**, *33*, 2908-2916.

(22) Huppert, J. L.; Balasubramanian, S. *Nucleic Acids Res.* **2007**, *35*, 406-413.

(23) Rodriguez, R.; Miller, K. M.; Forment, J. V.; Bradshaw, C. R.; Nikan, M.; Britton, S.; Oelschlaegel, T.; Xhemalce, B.; Balasubramanian, S.; Jackson, S. P. *Nat. Chem. Biol.* **2012**, *8*, 301-310.

(24) Doria, F.; Nadai, M.; Sattin, G.; Pasotti, L.; Richter, S. N.; Freccero, M. *Org. Biomol. Chem.* **2012**, *10*, 3830-3840.

(25) Röger, C.; Würthner, F. *J. Org. Chem.* **2007**, *72*, 8070-8075.

(26) Würthner, F.; Ahmed, S.; Thalacker, C.; Debaerdemaeker, T. *Chem.-Eur. J.* **2002**, *8*, 4742-4750.

(27) Zheng, K. W.; Zhang, D.; Zhang, L. X.; Hao, Y. H.; Zhou, X.; Tan, Z. *J. Am. Chem. Soc.* **2011**, *133*, 1475-1483.

(28) Doria, F.; di Antonio, M.; Benotti, M.; Verga, D.; Freccero, M. *J. Org. Chem.* **2009**, *74*, 8616-8625.

(29) Thalacker, C.; Roger, C.; Wurthner, F. *J. Org. Chem.* **2006**, *71*, 8098-8105.

(30) Suraru, S. L.; Wurthner, F. *J. Org. Chem.* **2013***, 78,* 5227−5238.

(31) Bhosale, R.; Perez-Velasco, A.; Ravikumar, V.; Kishore, R. S. K.; Kel, O.; Gomez-Casado, A.; Jonkheijm, P.; Huskens, J.; Maroni, P.; Borkovec, M.; Sawada, T.; Vauthey, E.; Sakai N.; Matile, S. *Angew. Chem. Int. Ed.* **2009***, 48,* 6461 –6464.

(32) Rogers, J. E.; Weiss, S. J.; Kelly, L. A. *J. Am. Chem. Soc.* **2000***, 122,* 427-436.

(33) Bhosale, S.; Sisson, A. L.; Talukdar, P.; Furstenberg, A.; Banerji, N.; Vauthey, E.; Bollot, G.; Mareda, J.; Roger, C.; Wurthner, F.; Sakai, N.; Matile, S. *Science* **2006**, *313*, 84-86.

(34) Guo, S.; Wu, W.; Guo, H.; Zhao, J. *J. Org. Chem.* **2012**, *77*, 3933-3943.

(35) Ajayakumar, M. R.; Asthana, D.; Mukhopadhyay, P. *Org. Lett.* **2012**, *14*, 4822-4825.

(36) Di Antonio, M.; Doria, F.; Mella, M.; Merli, D.; Profumo, A.; Freccero, M. *J. Org. Chem.* **2007**, *72*, 8354-8360.

(37) Guha, S.; Goodson, F. S.; Corson, L. J.; Saha, S. *J. Am. Chem. Soc.* **2012**, *134*, 13679-13691.

(38) Fin, A.; Petkova, I.; Doval, D. A.; Sakai, N.; Vauthey, E.; Matile, S. *Org. Biomol. Chem.* **2011**, *9*, 8246-8252.

(39) Mosinger, J.; Micka, Z. *J. Photochem. Photobiol. A* **1997**, *107*, 77-82.

(40) Wilkinson, F.; Helman, W. P.; Ross, A. B. *J. Phys. Chem. Ref. Data* **1993***, 22,* 113-262.

(41) Takizawa, S. Y.; Aboshi, R.; Murata, S. *Photochem. Photobiol. Sci.* **2011**, *10*, 895-903.

(42) Dy, J. T.; Ogawa, K.; Satake, A.; Ishizumi, A.; Kobuke, Y. *Chem.-Eur. J.* **2007**, *13*, 3491-3500.

(43) Pehrsson, L.; Ingman, F.; Johansson, A. *Talanta* **1976**, *23*, 769-780.

(44) Gans, P.; Sabatini, A.; Vacca, A. *Talanta* **1996**, *43*, 1739-1753.